

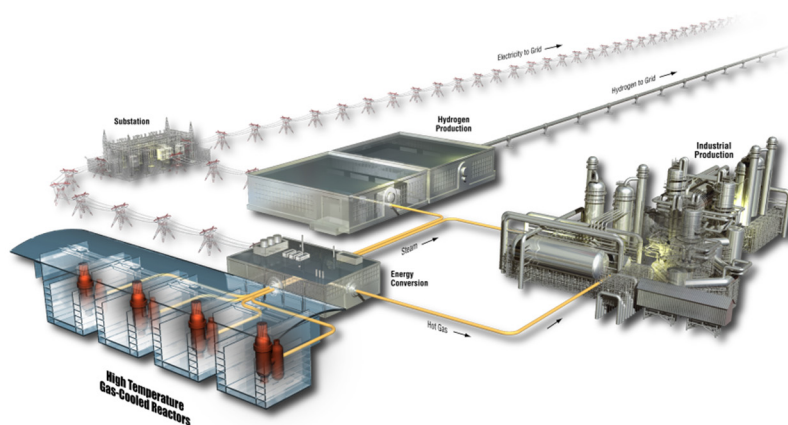
# Notch Effects on the Short-Term Rupture Properties of Alloy 617 Base Metal and Weldments

Project No.(s) 23747, 29412

Michael McMurtrey

September 2018

The INL is a  
U.S. Department of Energy  
National Laboratory  
operated by  
Battelle Energy Alliance



#### **DISCLAIMER**

This information was prepared as an account of work sponsored by an agency of the U.S. Government. Neither the U.S. Government nor any agency thereof, nor any of their employees, makes any warranty, expressed or implied, or assumes any legal liability or responsibility for the accuracy, completeness, or usefulness, of any information, apparatus, product, or process disclosed, or represents that its use would not infringe privately owned rights. References herein to any specific commercial product, process, or service by trade name, trade mark, manufacturer, or otherwise, does not necessarily constitute or imply its endorsement, recommendation, or favoring by the U.S. Government or any agency thereof. The views and opinions of authors expressed herein do not necessarily state or reflect those of the U.S. Government or any agency thereof.

# **Notch Effects on the Short-Term Rupture Properties of Alloy 617 Base Metal and Weldments**

**Michael McMurtrey**

**September 2018**

**Idaho National Laboratory  
INL ART Program  
Idaho Falls, Idaho 83415**

**<http://www.inl.gov>**

**Prepared for the  
U.S. Department of Energy  
Office of Nuclear Energy  
Under DOE Idaho Operations Office  
Contract DE-AC07-05ID14517**





## INL ART Program

# Notch Effects on the Short-Term Rupture Properties of Alloy 617 Base Metal and Weldments

INL/EXT-18-51278  
Revision 0

September 2018

**Author:**



Michael D. McMurtrey  
High Temperature Materials Researcher

9/5/18

Date

**Technical Reviewer:**



Richard N. Wright  
High Temperature Materials R&D Lead

09/05/2018

Date

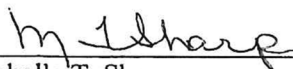
**Approved by:**



Diane V. Croson  
INL ART Deputy Director

9/5/18

Date



Michelle T. Sharp  
INL Quality Assurance

9/5/18

Date



## **ABSTRACT**

Alloy 617 is currently undergoing approval for inclusion in the American Society of Mechanical Engineers Boiler and Pressure Vessel Code in Section III Division 5 for use in high temperature nuclear reactors. Prior to use in construction of these reactors, however, designs incorporating this alloy must be approved by the Nuclear Regulatory Commission. Several concerns relating to the effects of geometric discontinuities, such as notches and multi-axial stress states (as opposed to uniaxial stress states typically present in laboratory run creep tests), must first be addressed. Alloy 617 has been found to be notch-strengthening in short-term (1,000-2,500 hour) creep testing for both base metal and weld metal and will fail preferentially in a straight gauge section rather than at a sharp notch, provided that the applied stresses are similar in both the straight gauge and notch sections. Additionally, specimens designed with semi-circular notches (or U-notches, as they are referred to in this report) to impose multi-axial stress states on the specimen during creep-testing were found to either maintain similar creep-rupture-lives as uniaxial stress specimens tested at similar conditions, or have creep-rupture-lives that were significantly longer. This work shows that notches and multi-axial stress states do not appear to raise concerns with relation to the use of design rules created for Alloy 617 using smooth, straight-gauge test specimens and uniaxial creep tests.



# CONTENTS

ABSTRACT.....	v
ACRONYMS.....	xi
1. INTRODUCTION.....	1
2. EXPERIMENTAL PROCEDURE.....	1
3. RESULTS AND DISCUSSION.....	8
3.1 Creep Results .....	8
3.1.1 V-notch .....	8
3.1.2 U-notch .....	10
3.1.3 Larson-Miller .....	12
3.2 Microscopy.....	13
3.2.1 V-notch .....	13
3.2.2 U-notch .....	16
3.3 Long Term Testing and Reference Short Term Specimens .....	25
4. CONCLUSIONS .....	27
5. ACKNOWLEDGMENTS .....	27
6. REFERENCES .....	28

# TABLES

Table 1. Chemical Composition of the Alloy 617 Plate and weld wire (weight percent).....	3
--	---

# FIGURES

Figure 1. INL Procedure Qualification Record sheets for Alloy 617 GTAW weld.....	5
Figure 2. Macrograph of the completed weld of Alloy 617 plate. ....	5
Figure 3. Micrographs of the qualified weld metal and adjacent base metal.....	6
Figure 4. Actual V-notch and U-notch specimens used in testing of notch effects: (a) V-notch specimen, (b) large radius U-notch specimen, (c) small radius U-notch specimen.....	7
Figure 5. Schematic of the Bridgeman notches with varying $d_{n0}/r_{n0}$ ratios. D is the outer diameter of the gauge, the $d_{n0}/r_{n0}$ ratios, and $r_{n0}$ is the radius of the notch itself. All notches in the schematic have a $D/d_{n0}$ value of $\sqrt{2}$ . ....	8
Figure 6. Creep results for V-notch specimens with extensometers over the straight-gauge section and tested at (a) 750°C, (b) 800°C, and (c) 900°C. ....	9
Figure 7. Creep results for V-notch specimens with extensometers across the V-notch. ....	9
Figure 8. Creep results for weld metal V-notch specimens, with extensometer over the straight gauge portion of the specimen. ....	10

Figure 9. Displacement vs time for creep tests of (a) large and (b) small radius U-notch specimens.....	11
Figure 10. Comparison of creep rates between base and weld metal for large radius U-notch specimens.....	12
Figure 11. Weld metal U-notch creep curves, showing large radius (left) and small radius (right) specimen results.....	12
Figure 12. The Larson-Miller plot, combining stress, temperature, and rupture time of the V-notch and U-notch (base and weld metal) tests for comparison with other 617 creep-rupture data [1]. ....	13
Figure 13. EBSD map showing grains near a V-notch tip. ....	14
Figure 14. EBSD map showing local misorientation (evidence of deformation) at varying locations of a specimen interrupted just prior to failure (750°C, 145 MPa). ....	15
Figure 15. Local misorientation data near the V-notch (distance 0) towards the center of the specimen (~1000µm into the specimen) from all tests characterized. The first two data sets (black and green) are not taken from the V-notch area, but rather taken from the interrupted test at the shoulder (no deformation) and straight-gauge (high levels of deformation). ....	16
Figure 16. Optical micrographs of cross sections from three base metal U-notch creep-rupture test specimens: (a),(b) small radius specimen tested at 800°C, 80 MPa; (c),(d) large radius specimen tested at 800°C 80 MPa; and (e),(f) large radius specimen tested at 900°C 36 MPa.....	17
Figure 17. EBSD local misorientation analysis of the small radius U-notch specimen tested at 800°C, 80 MPa. ....	18
Figure 18. EBSD local misorientation analysis of the large radius U-notch specimen tested at 800°C, 80 MPa. ....	18
Figure 19. Example of mesh used in finite element analysis. ....	19
Figure 20. Mean stress after creep has occurred, as calculated for a 750°C 145 MPa creep test. The maximum value is circled.....	20
Figure 21. Effective, or Von Mises stress after creep has occurred, as calculated for a 750°C 145 MPa creep test. The maximum value is circled. ....	20
Figure 22. Triaxiality ratio after creep has occurred, as calculated for a 750°C 145 MPa creep test. The maximum value is circled.....	21
Figure 23. Summary of modelled stress states for 750°C, 145 MPa condition. Solid lines indicate values upon loading the specimen, dashed lines indicate values after creep has occurred. ....	21
Figure 24. Graphical depiction of the process to determine void fraction (creep damage) vs. depth in the specimen cross section.....	22

Figure 25. Results of creep damage analysis for base metal, small radius U-notch specimens.....	23
Figure 26. Results of creep damage analysis for base metal, large radius U-notch specimens. ....	24
Figure 27. Optical micrograph of an etched cross section from a weld metal large radius U-notch specimen. ....	25
Figure 28. X-ray CT results showing (a) the entire reconstructed specimen, (b) and (c) the circumferential cross section near the rooth of the notch and (d) the longitudinal cross section. Cross sections were taken from the 3D reconstruction of the X-ray CT results while the specimen remained intact.....	26
Figure 29. X-ray CT results for the short term weld metal V-notch specimen (a and b) and the base metal long term V-notch specimen (c and d). Both samples are within 5-10% of their expected lives. ....	26





## ACRONYMS

ASME	American Society of Mechanical Engineers
ASTM	American Society for Testing and Materials
BPVC	Boiler and Pressure Vessel Code
CT	computed tomography
EBSD	electron backscatter diffraction
GTAW	gas tungsten arc welding
INL	Idaho National Laboratory
LMP	Larson-Miller parameter
NRC	Nuclear Regulatory Committee
SEM	scanning electron microscope
VDM	Vereinigte Deutsche Metallwerke – Company name
VHTR	very high temperature reactor



# Notch Effects on the Short-Term Rupture Properties of Alloy 617 Base Metal and Weldments

## 1. INTRODUCTION

The American Society of Mechanical Engineers (ASME) Boiler and Pressure Vessel Code (BPVC) Section III (Rules for Construction of Nuclear Facility Components), Division 5 (High Temperature Reactors) contains the design rules for components in high temperature nuclear reactors. This section of the BPVC also specifies those materials that are allowed for nuclear construction, contains the required material properties for design and construction, specifies welding processes that are acceptable, and specifies inspection requirements. There are a very limited number of materials for which sufficient high-temperature properties for design are available. The austenitic materials that are available for elevated temperature design are limited to Type 304 and Type 316 stainless steel and Alloy 800H.

Alloy 617 has been identified as the primary candidate material for the intermediate heat exchanger in very high temperature reactor (VHTR) concepts. This material exhibits good high-temperature mechanical properties that are minimally affected by long-term exposure to elevated temperatures. Recent testing in the United States, in collaboration with Generation IV International Forum partners and an extensive historical database, has been used to develop a draft Code Case for qualification of Alloy 617 in Section III, Division 5, of the BPVC [1]. Code qualification of this material will allow it to be used in nuclear construction up to 950°C and up to 100,000 hours.

The Nuclear Regulatory Commission (NRC), however, has not officially endorsed the design rules that are contained in Section III, Division 5, for use in VHTR construction. Potential application of these rules to elevated temperature nuclear designs, including the Clinch River Breeder Reactor, has been reviewed by the NRC and comments have been published and revisited several times [2]. These reviews have concluded that the impact of notches and structural discontinuities on the service behavior of components at elevated temperature has not been adequately addressed. Resolving these potential issues is a cross-cutting activity that can impact designs using any qualified high-temperature material. Alloy 617 has been chosen as the prototypical material to investigate these issues because of the vast amount of readily available material property data that are available as a result of preparing the Code Case.

Extensive characterization of Alloy 617 high-temperature properties has been carried out under laboratory conditions using uniaxial loading conditions for both base and welded plate material. This testing has included determination of the mechanism responsible for steady-state or minimum creep rate, measurement of creep-rupture behavior over a wide range of stresses and temperatures, and examination of the relationship between onset of tertiary creep and cavity formation. Despite the fact that uniaxial testing is exclusively used in determining time-dependent allowable stresses for ASME design purposes, relevant components operate under multi-axial stress states in service. Thus, it is desirable to examine behavior of high-temperature materials under multi-axial conditions, and compare the behavior to standard uniaxial laboratory tests. Testing of multi-axial stress state effects was performed, according to Idaho National Laboratory (INL) document PLN-5086 [3]. This report covers the results of the short-term testing of base and weld metal, as well as the plans and preliminary results for long term testing.

## 2. EXPERIMENTAL PROCEDURE

Specimens were machined with their longitudinal axes oriented along the rolling direction from a 37 mm thick solution annealed plate provided by ThyssenKrupp VDM (Heat #314626) Composition of this plate is given in Table 1, along with the ASME specified chemistry. This is the same material used in the Code Case studies and developing the steady-state creep rate equations and the Larson-Miller equations to describe rupture behavior. The average grain size (as measured by the linear intercept method) is 150  $\mu\text{m}$ . Carbide banding and stringers parallel to the rolling direction are also present in the as-received

microstructure. The bands are approximately 100-300  $\mu\text{m}$  wide, and the carbides appear to form on a prior grain structure, which are finer and unrelated to the present grain boundary structure. Outside of these banded regions, there are few secondary particles, with the exception of a small number of titanium nitrides.

Table 1. Chemical Composition of the Alloy 617 Plate and weld wire (weight percent).

Heat ID	Source	Form	Ni	Cr	Co	Mo	Fe	Mn	Al	C	Cu	Si	S	Ti	B
	ASME		44.5 min	20.0- 24.0	10.0- 15.0	8.0- 10.0	3.0 max	1.0 max	0.8- 1.5	0.05- 0.15	0.5 max	1.0 max	0.015 max	0.6 max	0.006 max
314626	VDM	plate	54.1	22.2	11.6	8.6	1.6	0.1	1.1	0.05	0.04	0.1	<0.002	0.4	<0.001
XX3703UK	Oxford	weld wire	53.91	22.41	11.49	8.98	1.37	0.11	1.10	0.089	0.04	0.04	0.001	0.34	NR

A qualified weld was constructed from the INL Alloy 617 plate for use in weld metal and adjacent heat affected zone studies. The INL has performed extensive property characterization on specimens machined from this reference material. The weld wire was ERNiCrCoMo-1 (Alloy 617), (heat XX3703UK) produced by Oxford Alloys. The chemical composition for the weld wire is shown in Table 1. Welding was performed using an automated gas tungsten arc welding (GTAW) process with multiple passes to fill a V-notch weld preparation.

The GTAW process was qualified for 1.5 inch thick plate using the ERNiCrCoMo-1 (Alloy 617) filler metal and the ASME Section IX qualification process through the INL Welding Procedure Specification I5.0. The INL Procedure Qualification Record sheets are shown in Figure 1. The properties of the weld were qualified using tensile and bend testing, the results of which are reported on page 2 of the Procedure Qualification Record. No post-weld heat treatment is required for Alloy 617, and all characterization was done in the as-welded condition.

A macrograph showing the completed weld is shown in Figure 2. Micrographs of a polished and etched cross-section of the weld are shown in Figure 3. It can be seen in the micrographs that there is no heat affected zone associated with this GTAW weldment, as expected for a solid solution austenitic alloy.

Welds that were produced using this procedure for subsequent rupture and notch testing passed examination using the criteria in Section III Division 5 HBB-5210 (b), including radiographic examination using two different angles.

IDAHO NATIONAL LABORATORY PROCEDURE QUALIFICATION RECORD		Page 1 of 2 REV NO.: 0
CODE: ASME IX-QW PQR NO.: WPD 656		
COMPANY NAME: INL PQR NUMBER: WPD 656 WELDING PROCESS: GTAW		DATE: 8/5/09 REVISION: 0 TYPES: Machine
<b>JOINT (QW-402)</b> 		<b>POST WELD HEAT TREATMENT (QW-407)</b> TEMPERATURE: NA TIME: NA <b>GAS (QW-408)</b> SHIELDING: Helium/Argon COMPOSITION: 75% / 25% Welding Grade FLOW RATE: 30 cfh PURGING: NA COMPOSITION: NA FLOW RATE: NA TRAILING: NA COMPOSITION: NA FLOW RATE: NA
<b>BASE METALS</b> SPECIFICATION: ASME SB 168 TYPE OR GRADE: Alloy 617 UNS N06617 P NO. FROM: 43 THICKNESS: 1.500 in. OTHER: NA		TO P NO.: 43 DIAMETER: NA <div style="border: 2px solid red; padding: 5px; color: red; font-weight: bold; text-align: center;">CONTROLLED COPY</div>
<b>FILLER METALS</b> SPECIFICATION: SFA 5.9 CLASSIFICATION: ERNiCrCoMo-1 F NO.: 6 SOLID/TUBULAR/FLUX/COVERED/GTAW: Solid SIZE: 0.045 in. CHEMICAL COMPOSITION: NA OTHER: NA		
<b>POSITION (QW-405)</b> POSITION: 1G PROGRESSION: NA		<b>PREHEAT (QW-406)</b> PREHEAT TEMP. (MIN): 50° F INTERPASS TEMP. (MAX): 200° F
<b>ELECTRICAL CHARACTERISTICS (QW-409)</b> CURRENT: Direct POLARITY: Straight AMPS: 200 to 355 VOLTS: 9 to 13 TUNGSTEN TYPE: EWTh-2 TUNGSTEN SIZE: 0.125 in.		<b>TECHNIQUE (QW-410)</b> TRAVEL SPEED: 3.5 to 5 ipm STRING OR WEAVE BEAD: Stringer and weave OSCILLATION: Slight SINGLE/MULTIPLE PASS: Multiple SINGLE/MULTIPLE ELEC.: Single TRANSFER MODE(GMAW): NA

TENSILE TEST (QW-150)						
SPECIMEN NUMBER	WIDTH (mm)	THICK. (mm)	AREA (mm <sup>2</sup> )	LOAD (Kn)	UTS (ksi)	TYPE OF FAILURE AND LOCATION
A-Q-1	18.99	11.71	222.4	161.2	118	Ductile / BM
A-Q-2	18.63	11.79	219.7	175.7	116	Ductile / BM
A-MID	19.01	11.47	218.0	170.2	113	Ductile / BM
B-Q-1	18.56	11.42	212.0	174.5	119	Ductile / Weld
B-Q-2	18.95	11.49	217.7	175.1	117	Ductile / BM
B-MID	18.62	10.98	204.5	166.3	118	Ductile / BM

GUIDED BEND TESTS (QW-160)	
TYPE AND FIGURE NUMBER	RESULTS
Side bends 4 EA, Figure QW 462.2	Pass

NOTES:

CONTROLLED COPY

WELDER'S NAME: Denis Clark      IDENTIFICATION: KI

TEST BY: Kyle Kofford

WE CERTIFY THAT THE STATEMENTS IN THIS RECORD ARE CORRECT AND THAT THE TEST WELDS WERE PREPARED, WELDED, AND TESTED IN ACCORDANCE WITH THE REQUIREMENTS OF SECTION IX OF THE ASME 2007 CODE.

CERTIFIED BY: *Michael Clark*

COMPANY: INL

DATE: 2/2/09

Figure 1. INL Procedure Qualification Record sheets for Alloy 617 GTAW weld.



Figure 2. Macrograph of the completed weld of Alloy 617 plate.

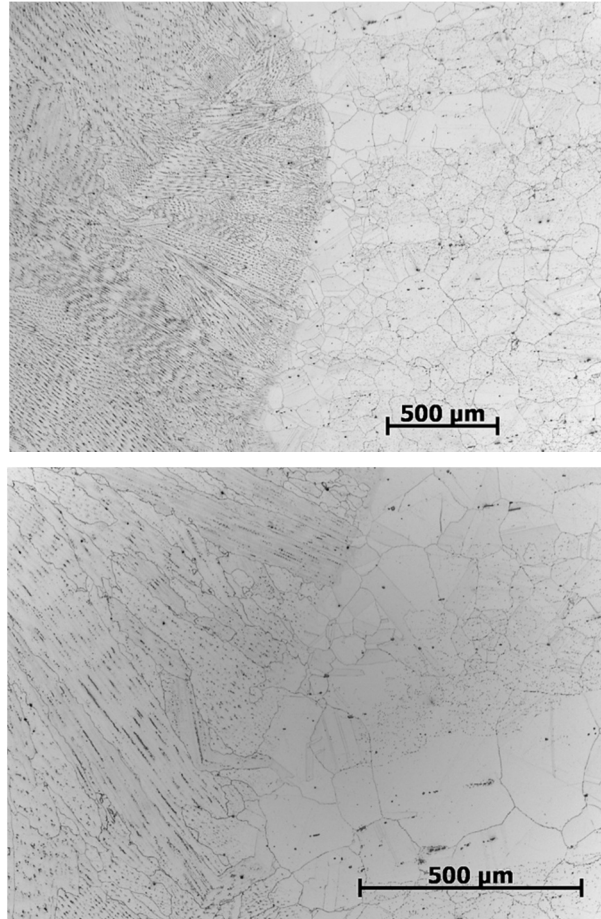


Figure 3. Micrographs of the qualified weld metal and adjacent base metal.

Three general specimen geometries were examined in this work for both base metal and weld metal specimens. Two were characterized as U-notch specimens, with semi-circular notches, differing only in the radii of the notches. The third type were V-notch specimens with both sharp notch (V-notch) and straight-gauge portions (the diameter of the straight-gauge section is the same as the diameter at the root of the notch). The V-notch specimens were used to determine if the material was notch strengthening, while the U-notch was used to examine the multi-axial creep response [4].

The V-notch specimen design is specified in American Society for Testing and Materials (ASTM) Standard E292-09 [5]. A small modification to the ASTM design was made to allow an extensometer to be connected to the specimen via grooves placed between the V-notch and the threads, the straight-gauge section and the V-notch, and the straight-gauge section and the threads, as seen in Figure 4a. This allows for displacement measures over the straight-gauge section, the V-notch, or the entire length of the specimen. The ASTM standard limits the use of the V-notch specimen to evaluating rupture behavior. This type of specimen was originally developed to describe the behavior of materials at the root of a thread. V-notch specimens are widely used to determine if a material at a particular temperature exhibits notch-strengthening or notch-weakening. The presence of both a standard straight-gauge section and a V-notch allow for comparison between a conventional creep test and a notched test. If the specimen fails at the V-notch, it is notch-weakening, if the failure occurs in the straight-gauge, it is notch-strengthening. The diameter at the straight-gauge section and at the root of the V-notch is 6.4 mm, similar to the sizes of straight-gauge creep specimens tested previously at INL, allowing for direct comparisons between the previous and current work. For the weld metal, the specimen was cut along the length of the weld, such



that the entire specimen was machined from weld metal (ensuring that both the V-notch and the straight gauge were weld metal).

Two different U-notch specimens, as shown in Figure 4b and Figure 4c for the base metal (the weld metal specimens were limited to a single notch), were machined; one with a  $d_{n0}/r_{n0}$  ratio of 1 and the other with a ratio of 4.83, as shown in Figure 5. The ratio of the outer and inner diameters of the specimen (e.g.,  $D/d_{n0}$  in Figure 5) is arbitrary, however, a ratio of  $\sqrt{2}$  has been used extensively with this specimen design and is recommended by the Code of Practice [4]. U-notch specimens are commonly used for notch/multi-axial stress effects on creep behavior. The double notch in the base metal specimens allows for the examination of the failure mechanism for one of the notches, and the remaining, unfailed notch may be sectioned for metallographic analysis of the state just prior to failure. The welded specimens were machined perpendicular to the weld, such that the notch is weld metal and the threads are base metal. Given the narrowness of the weld, it was not possible to machine the specimens with two notches that were both contained within the weld metal area. The ratio of the diameter across the specimen at the root of the notch and the radius of the notch (e.g.,  $d_{n0}/r_{n0}$  in Figure 5) defines the severity of the notch and the resulting multi-axial stress state at the root of the notch. A ratio of 4.83 is the maximum that can be obtained, while still maintaining a semi-circular notch.

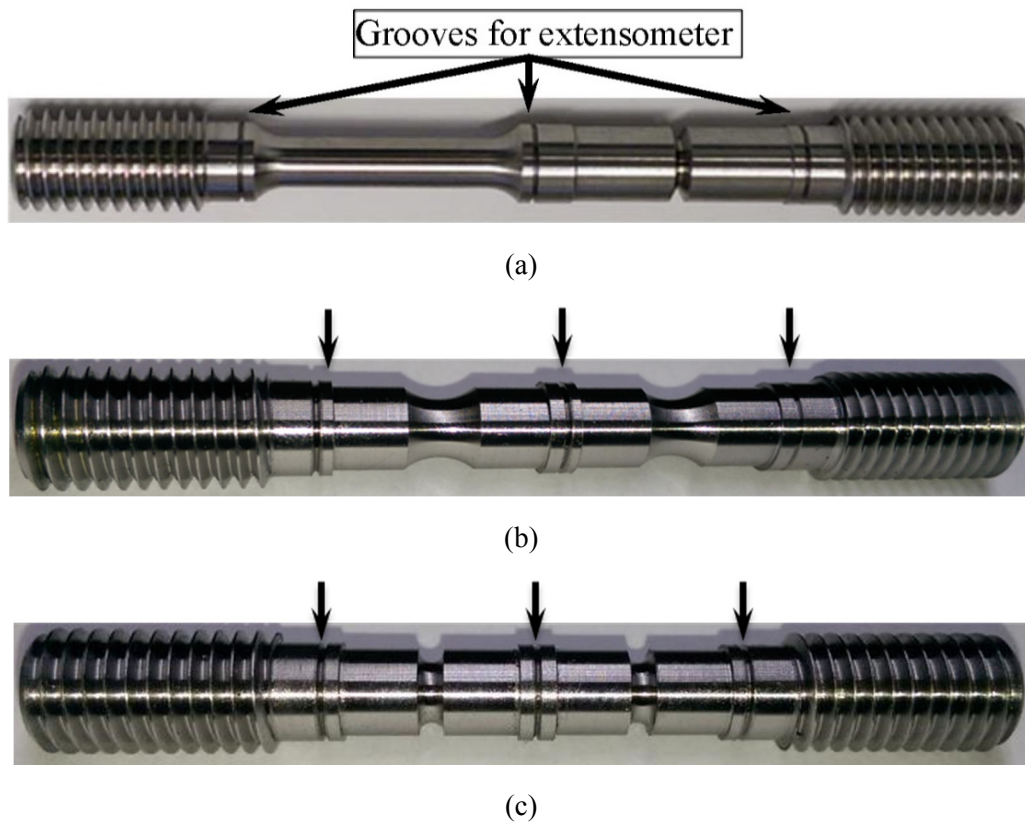


Figure 4. Actual V-notch and U-notch specimens used in testing of notch effects: (a) V-notch specimen, (b) large radius U-notch specimen, (c) small radius U-notch specimen.

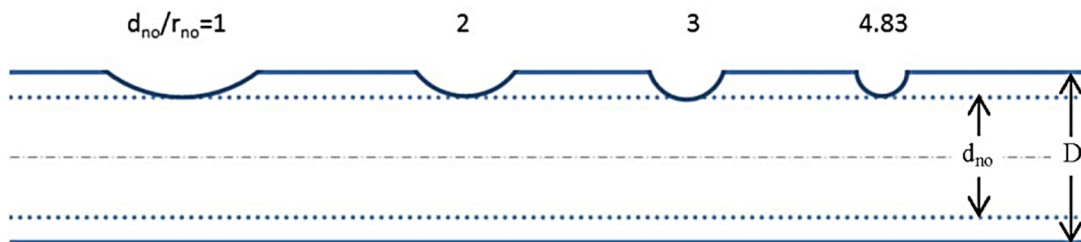


Figure 5. Schematic of the Bridgeman notches with varying  $d_{n0}/r_{n0}$  ratios.  $D$  is the outer diameter of the gauge, the  $d_{n0}/r_{n0}$  ratios, and  $r_{n0}$  is the radius of the notch itself. All notches in the schematic have a  $D/d_{n0}$  value of  $\sqrt{2}$ .

Creep-testing has been carried out over a range of temperatures, from 750°C up to 1,000°C. Stresses were chosen such that tests were completed within a reasonable amount of time (~1,000–2,000 hours) based on the Larson-Miller analysis for base metal and ranged from 20 to 225 MPa. In general, preference was given to test conditions that matched conditions for conventional creep tests run previously at INL for comparison. The testing conditions have been modified since the original test plan [3] in order to match prior work more closely. Following rupture, select specimens were cross-sectioned for micrographic analysis at both the straight-gauge section and the V-notch, or both the ruptured and intact U-notch. In addition to the metallographic preparation of cross-sections, some specimens were electrochemically polished and then electrochemically etched to reveal grain boundaries using perchloric acid at 0°C and at a potential of 24V for electropolishing followed by electroetching at 9V using a Struers LectroPol 5. Additionally, some specimens were characterized using electron backscatter diffraction (EBSD) in a Joel 650 scanning electron microscope (SEM). EBSD provides information on grain size/orientation and, by examining small changes to the local misorientation of the crystal lattice, can provide some qualitative information on deformation, highlighting areas of high amounts of deformation.

### 3. RESULTS AND DISCUSSION

Short-term testing has been completed for base metal, with some short-term weld metal testing still ongoing or planned. Results show that Alloy 617, at the conditions tested, is notch strengthening, and that there is no life shortening due to the presence of multi-axial stress states. A detailed analysis of the results is presented in the section showing creep results then microscopy, with V-notch results first, followed by the U-notch testing results. In addition to the short-term results, there will be some discussion of the ongoing long term testing. While not the focus of this report, the long term testing is informed by the short-term results.

#### 3.1 Creep Results

##### 3.1.1 V-notch

Seven base metal creep-rupture tests were completed on V-notch specimens, including replicates of all conditions, with the exception of the 1,000°C and 20 MPa test, where the temperature control failed during the replicate test, so the results were not included. All tests resulted in rupture in the straight-gauge portion of the specimen rather than the V-notch, showing that, at these conditions, Alloy 617 is notch-strengthening.

Creep curves for the V-notch specimens, with displacement measured with extensometers over the straight-gauge section, are shown in Figure 6. Also included in each of the graphs in Figure 6 are the curves from prior creep tests with straight-gauge specimens performed at INL with the same conditions. While variations in time to rupture are observed, the variations are within expectations based on the variability of measured creep properties reported in the ASTM E139-11 standard for conducting creep

tests of metallic materials [6]. Replicate tests were performed with the extensometer over the V-notch portion of the specimen. The results are shown in Figure 7. Note that the results in Figure 7 show displacement vs. time, rather than strain % vs. time, as is the case in Figure 6. This is due to the difficulty in assigning a gauge length for notched specimens, which is needed in order to calculate strain.

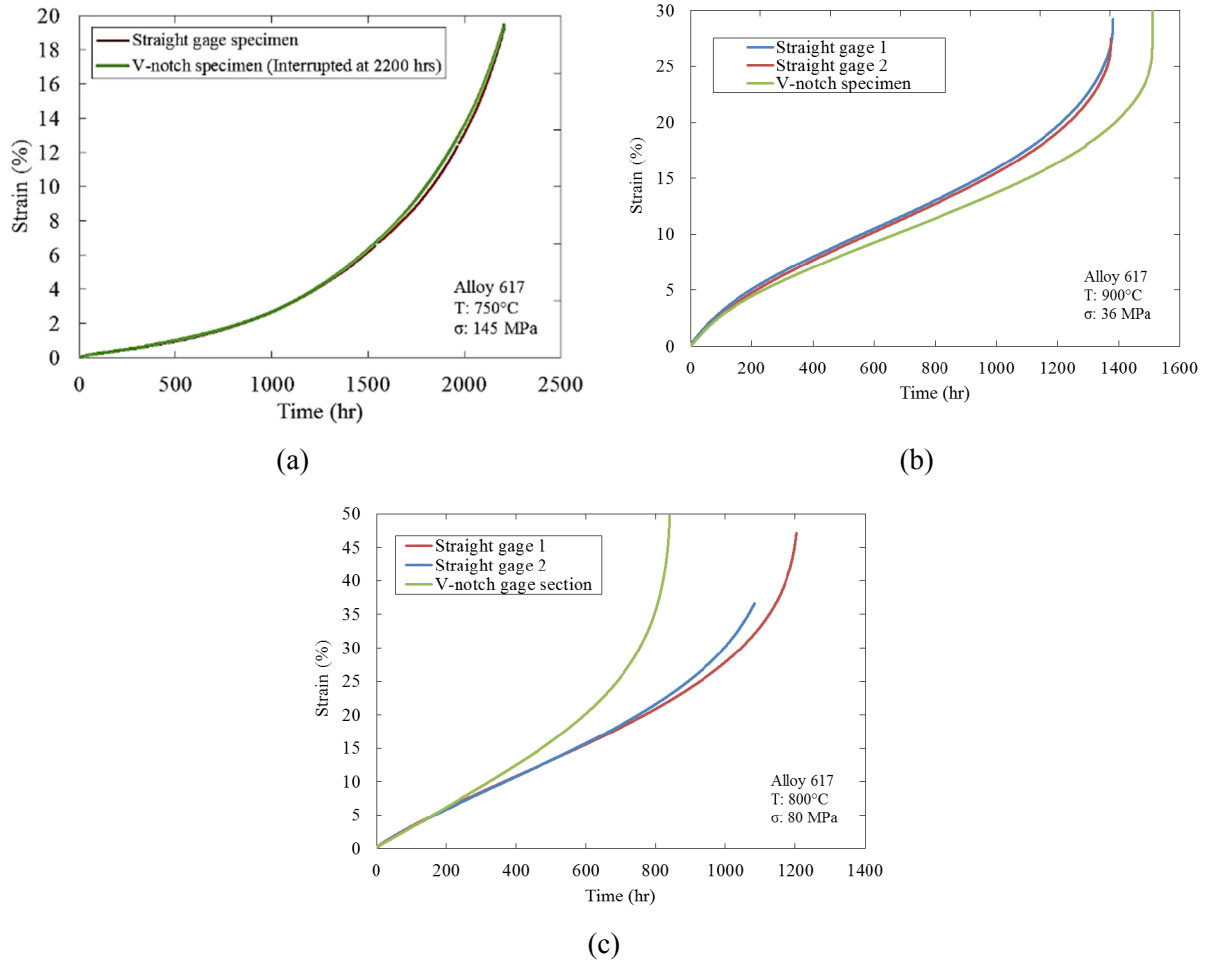


Figure 6. Creep results for V-notch specimens with extensometers over the straight-gauge section and tested at (a) 750°C, (b) 800°C, and (c) 900°C.

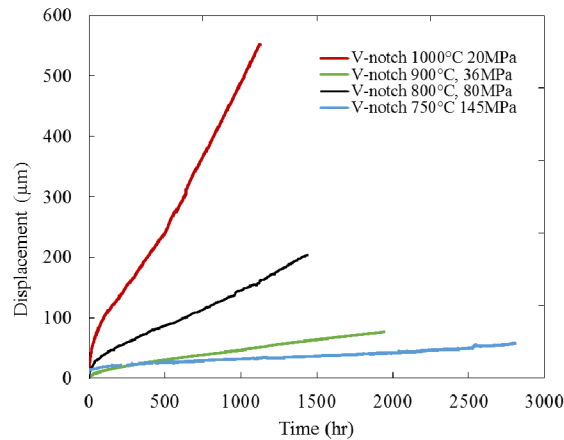


Figure 7. Creep results for V-notch specimens with extensometers across the V-notch.

One weld metal V-notch specimens have been tested to rupture and two are currently ongoing. Figure 8 shows the creep curves for the weld metal specimens, with the extensometer over the straight gauge portion of the specimens. The results from the 800°C and 110 MPa test are most closely comparable to the base metal results depicted in Figure 6c. The weld metal was found to exhibit a significant decrease in ductility over the base metal (20% strain in the weld metal at failure vs. the 50% of the base metal). The weld metal was expected to exhibit a longer creep life than the base metal, so a higher stress was chosen for the weld test. The ongoing tests include a long term test (~100,000 hour expected life) and a short-term test being used as a basis for the long term test, which will be discussed later in this report.

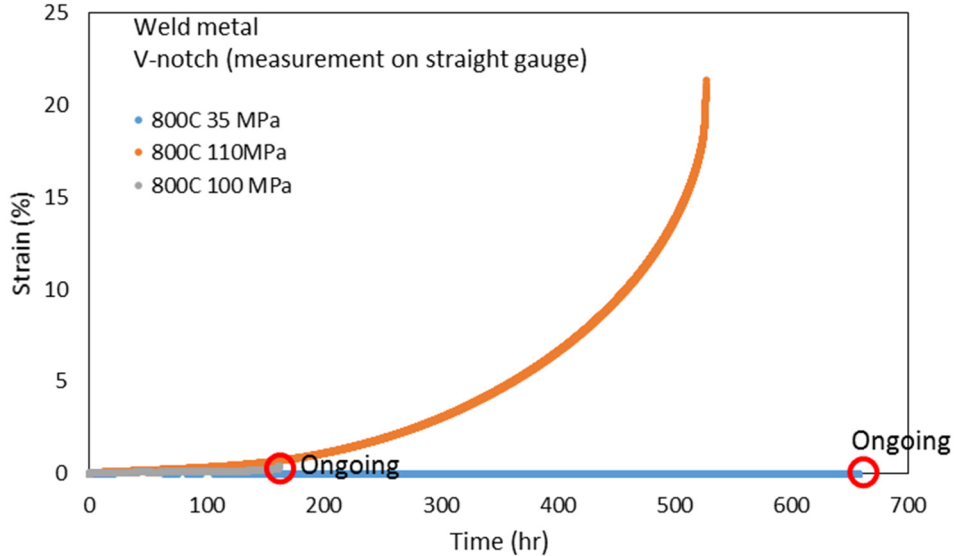
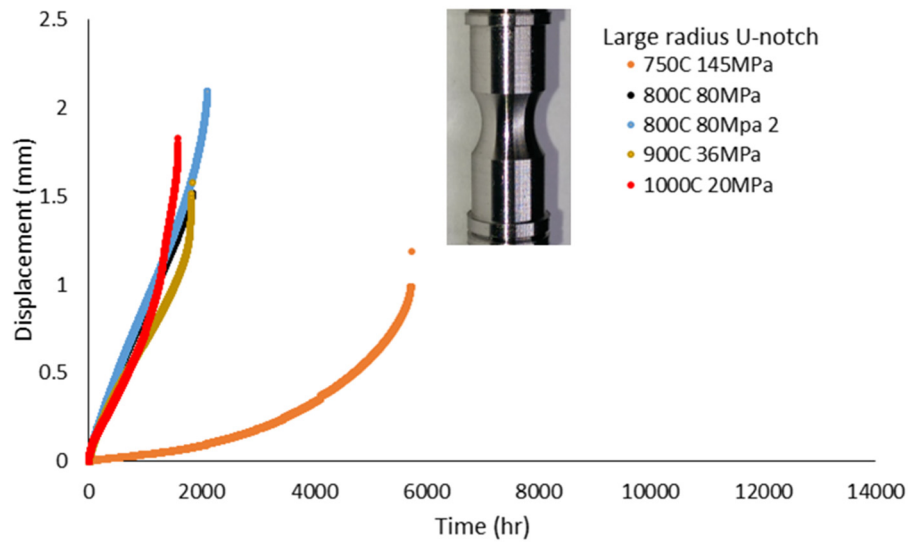


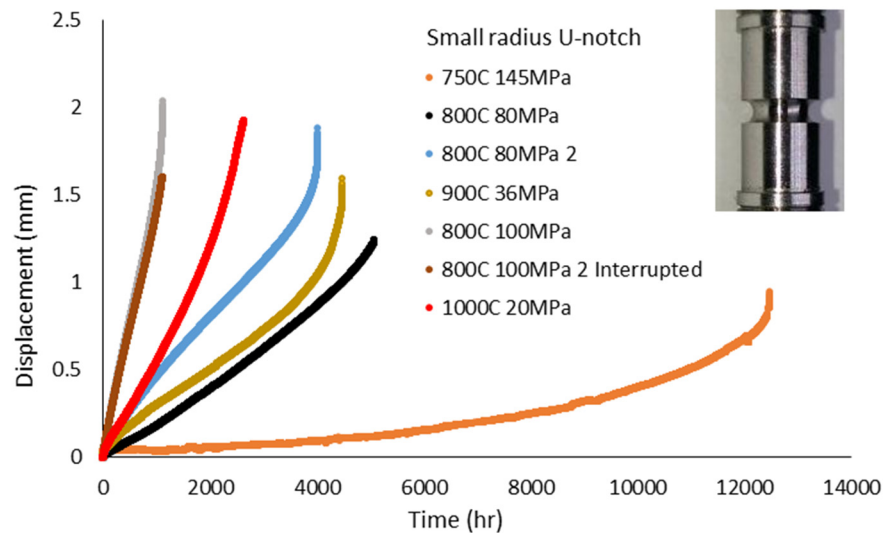
Figure 8. Creep results for weld metal V-notch specimens, with extensometer over the straight gauge portion of the specimen.

### 3.1.2 U-notch

A total of twelve base metal U-notch specimens were tested. Tests were performed at 750°C, 800°C, and 900°C, with a replicate test being performed at 800°C. Five base metal, large radius U-notch creep-rupture tests were also completed, with results shown in Figure 9a. Seven base metal, small radius U-notch creep-rupture tests were completed (one of which was a planned interrupted test and was not taken to failure), results are shown in Figure 9b. The interrupted and the ruptured specimen at the same conditions (800°C, 100 MPa) were sent to Argonne National Laboratory for additional characterization in the Advanced Photon Source to examine creep damage in failed notched specimens and at the onset of tertiary creep.



(a)



(b)

Figure 9. Displacement vs time for creep tests of (a) large and (b) small radius U-notch specimens.

Five weld metal U-notch specimens have been tested, with four tested until rupture, and one interrupted prior to completion. The interrupted test was the first weld metal test performed and was intended to give a general idea as to the creep rate of the weld metal and then be used to confirm through microscopy that the notch was entirely contained within the weld metal as expected. This was an important verification that needed to be performed prior to beginning the testing effort in earnest. The weld metal was found to have a much lower creep rate than the base metal, as seen in Figure 10. The creep curves for large and small radius U-notch specimens are shown in Figure 11. Similar to the V-notch results, the weld metal specimens were found to have a decreased ductility when compared to the base metal. The effects of notches and base vs. weld metal on creep rupture life will be discussed in the next section.

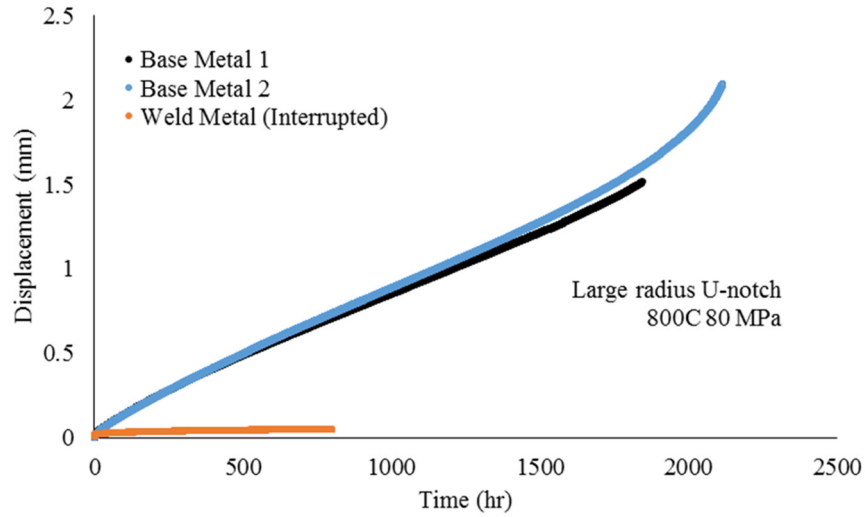


Figure 10. Comparison of creep rates between base and weld metal for large radius U-notch specimens.

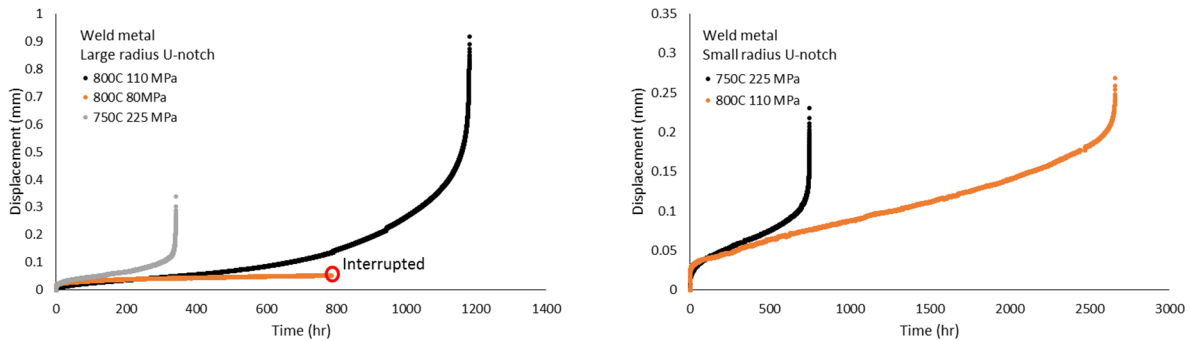


Figure 11. Weld metal U-notch creep curves, showing large radius (left) and small radius (right) specimen results

### 3.1.3 Larson-Miller

The Larson-Miller parameter (LMP) is a convenient way to compare creep-rupture data between samples at different loading stresses and temperatures. The LMP is defined as:

$$LMP = T(C + \log_{10}(t)) \quad [1]$$

where  $T$  is the absolute temperature,  $C$  is the Larson-Miller constant, and  $t$  is the time to rupture.

Figure 12 shows the results for base and weld metal for all of the V-notch tests and U-notch tests, as well as conventional creep-rupture data of base metal collected at INL from a number of sources and reported in the Code Case [1] included for comparison. The base metal V-notch specimens rupture-lives fall well within the spread of compiled straight gauge data in the Larson-Miller plots, showing that the presence of the V-notch had essentially no impact on the creep-rupture life, which was expected given that the material is notch strengthening and failure occurred in the straight gauge portion of the specimen. The single finished weld metal V-notch rupture test falls right on the calculated Larson Miller line, suggesting no difference in rupture life between the base metal and weld metal specimens.

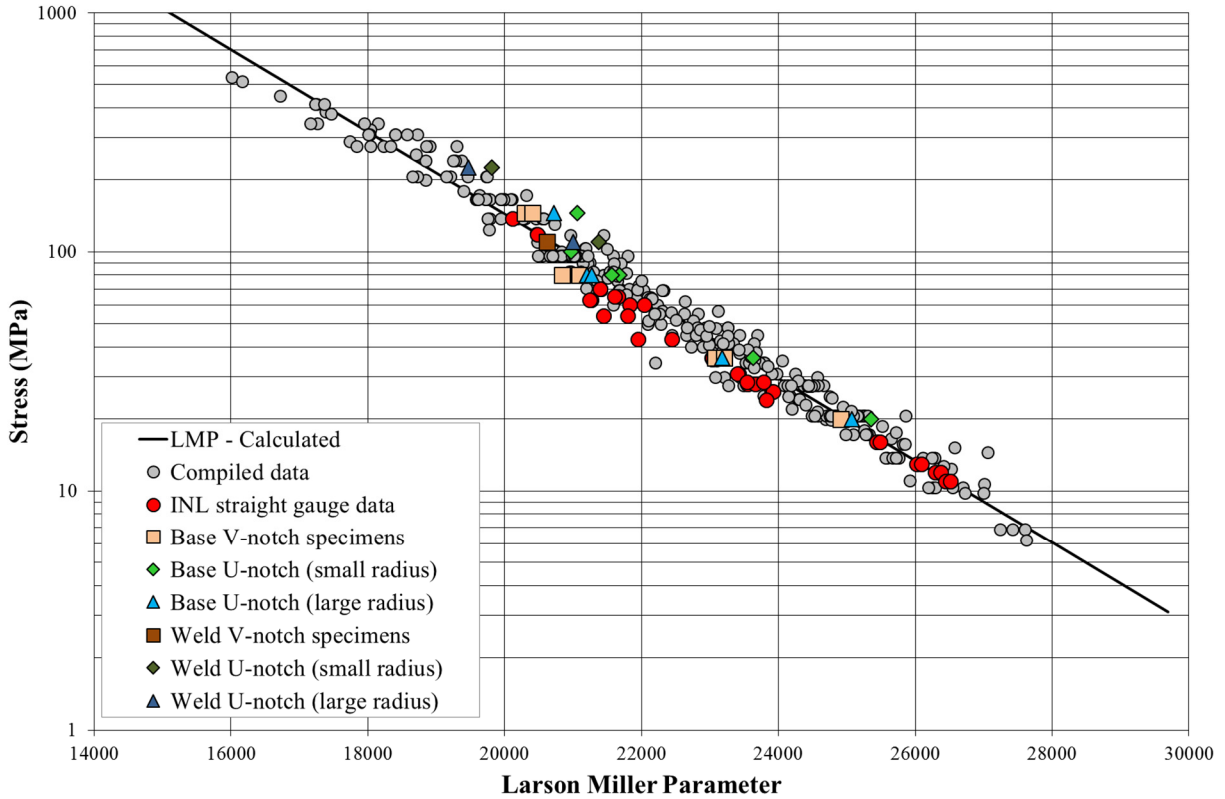


Figure 12. The Larson-Miller plot, combining stress, temperature, and rupture time of the V-notch and U-notch (base and weld metal) tests for comparison with other 617 creep-rupture data [1].

The base metal U-notch results are also shown in the Larson-Miller plot in Figure 12. Like the V-notch tests, these results currently all fall within the scatter of data; however, it is important to note that the small radius U-notch tests are all significantly further right than other tests performed at INL. This suggests that though they fall within the scatter of multi-facility/ multi-material heat test results (it may be argued that the 145 MPa, the green diamond at ~21,000 LMP, test falls to the right, outside of the scatter), they experience significantly longer creep-rupture-lives than other specimen geometries at similar conditions tested at INL, for the same heat of Alloy 617. The large radius U-notch, which imposes a small, diffuse multi-axial stress state throughout the thickness of the specimen acts very similar to the straight-gauge, uniaxial stress specimens previously tested. The small radius U-notch tests exhibit longer creep-rupture-lives. The weld metal U-notch specimens followed a similar trend, with all results falling within the scatter of data, though the small radius specimens always were on the rightmost edge of the scatter, due to their longer creep rupture life.

## 3.2 Microscopy

### 3.2.1 V-notch

Detailed optical micrographs of the first two ruptured V-notch specimens were reported previously [7]. All specimens tested were found to contain creep damage throughout both the entire thickness and length of the straight-gauge portion of the specimen. Only a small amount of damage was observed at the tip of the V-notch, with no additional damage observed elsewhere in the reduced gauge section of the V-notch portion of the specimen. Additional characterization of the damage around the V-notch was performed using EBSD analysis in a SEM.



EBSD results show that along the edge of the specimen, there is a  $\sim 20\mu\text{m}$  thick layer of small grains, which is a result of machining damage. An example of these small grains is shown in Figure 13, showing an area near the V-notch tip; however, these grains were apparent over the entire edge of the specimen, not just the V-notch. A more detailed EBSD analysis was performed to look at local misorientation of the lattice. Deformation can cause rotation of the crystal lattice (largely due to the presence of certain types of dislocations), which is visible when local misorientation is mapped using EBSD. A V-notch specimen was tested at  $750^\circ\text{C}$ , 145 MPa, and interrupted at 2,200 hours (prior to rupture). The specimen was cross-sectioned at both the V-notch and the straight-gauge. EBSD local misorientation measurements were taken to use as a baseline for qualitative comparisons of deformation near the V-notch of all the specimens. This was accomplished by taking measurements where no deformation was expected (e.g., the thick shoulder of the specimen) and measurements where significant deformation was known to have occurred, due to overall changes in the specimen measurements (e.g., the straight-gauge section). These were then compared to measurements taken around the V-notch to determine where deformation had occurred. Examples of the measurements that were taken are shown in Figure 14. Note the large amount of green in the measurements taken in the straight-gauge, showing significant local misorientation. Near the shoulder, the EBSD maps show mostly blue, indicating little to no local misorientation. All measurements near the edge (e.g., shoulder, straight-gauge, and V-notch) show a narrow bright green band along the edge, a result of the machining damage already discussed. Note in Figure 14 that the green areas (corresponding to certain grains) seen in the map taken near the V-notch tip are measurement artifacts of the measurement technique. This is why the entire grain appears a near uniform shade of green, rather than bright highlighted portions (generally highlighting grain boundaries and slip planes where deformation occurs) as seen in the high-deformation areas of the straight-gauge.

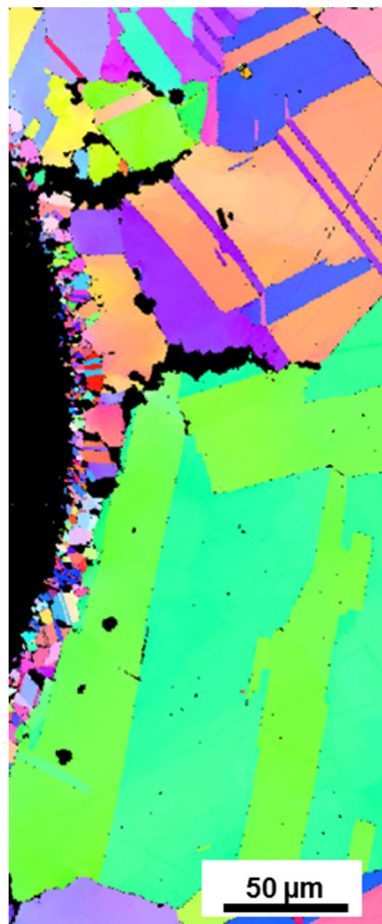


Figure 13. EBSD map showing grains near a V-notch tip.



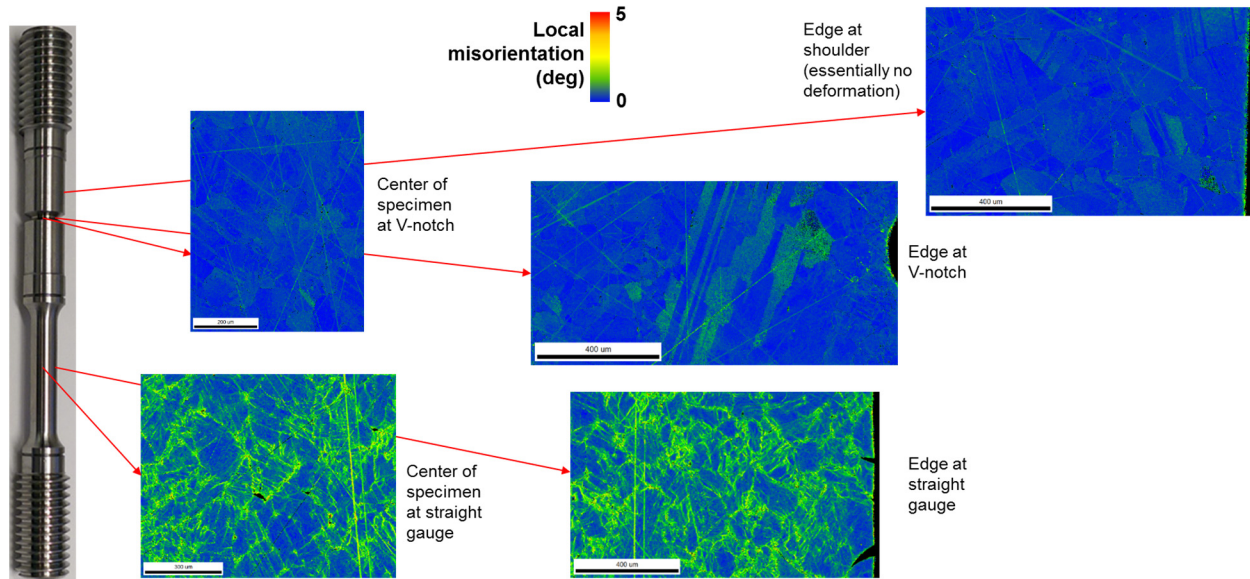


Figure 14. EBSD map showing local misorientation (evidence of deformation) at varying locations of a specimen interrupted just prior to failure (750°C, 145 MPa).

Local misorientation values were extracted from the EBSD maps, starting at the tip of the V notch and traveling towards the center of the specimen. The results for all analyzed specimens are shown in Figure 15. In this figure, distance 0 corresponds to the very tip of the V-notch. All measured specimens show a small,  $\sim 20\ \mu\text{m}$  peak at 0, which is a measurement of the machining damage already discussed. Measurements taken from the interrupted test, starting at the edge of the specimen and moving inwards from both the shoulder and the straight-gauge give examples how no deformation and high-deformation, respectively, would appear. All specimens, with the exception of the 750°C test, follow a similar trend. Deformation appears to be present up to  $\sim 150\ \mu\text{m}$ , at which point, the lines generally converge into the same area occupied by the “no deformation” (black) line. The 750°C measurements appear to follow the black line (with the exception of two plateaus, which represent the measurement artifacts previously discussed). These results show that there is essentially no deformation occurring in the specimen tested at 750°C, while the higher temperature specimen tests resulted in limited deformation that was constrained to the area within  $\sim 150\ \mu\text{m}$  of the V-notch tip.

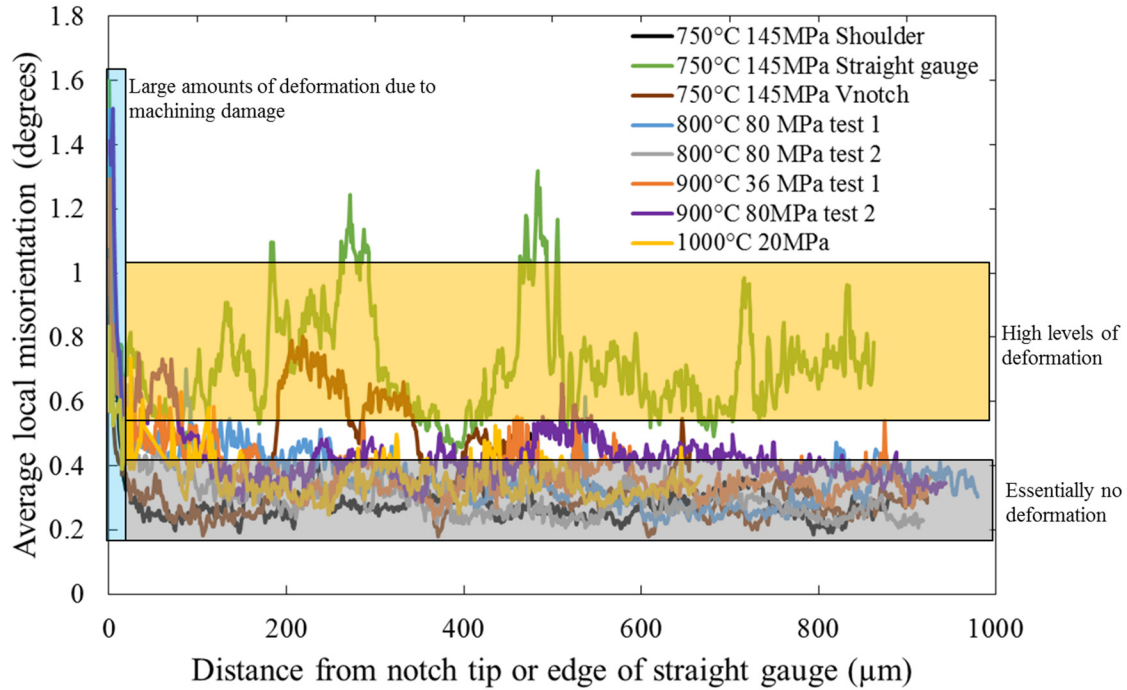


Figure 15. Local misorientation data near the V-notch (distance 0) towards the center of the specimen (~1,000 $\mu\text{m}$  into the specimen) from all tests characterized. The first two data sets (black and green) are not taken from the V-notch area, but rather taken from the interrupted test at the shoulder (no deformation) and straight-gauge (high levels of deformation).

The geometric constraints of the notch restrict the radial contraction that would occur in the area near the tip of the notch when the specimen plastically deforms and elongates. The constraints on the deformation are from the wider shoulders adjacent to the notch, which experience significantly lower levels of stress and thus are not inclined to deform and accommodate deformation at the tip notch [8,9]. The straight-gauge section has no such constraints and both elongates along the loading axis as well as radially contracts. As the test progressed, this means that an increased level of stress was experienced by the straight-gauge section, whereas the applied stress at the V-notch remained the same, due to the nature of the constant load test and the changing dimensions of the specimen.

### 3.2.2 U-notch

Cross-sectional analysis of three tested base metal specimens are shown in Figure 16. From the analysis of the unbroken notch (see Figure 16a, c, and e), creep damage is observed near the notch tip of the small radius specimen, while barely present near the center of the specimen. The large radius specimens show near uniform damage across the entire thickness of the gauge. The fractured notches (Figure 16b, d, and f) appear fairly similar between the two geometries.

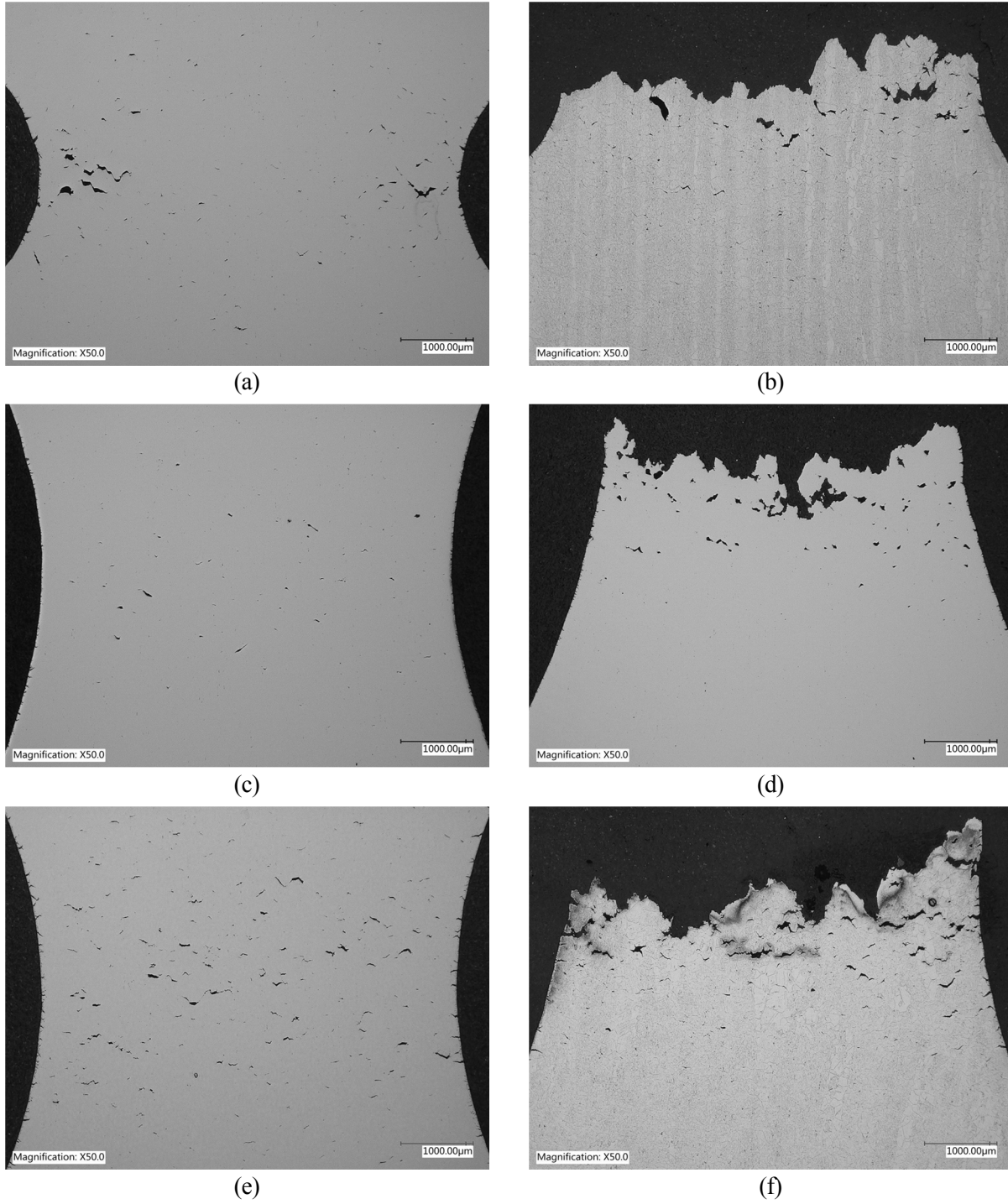


Figure 16. Optical micrographs of cross sections from three base metal U-notch creep-rupture test specimens: (a),(b) small radius specimen tested at 800°C, 80 MPa; (c),(d) large radius specimen tested at 800°C 80 MPa; and (e),(f) large radius specimen tested at 900°C 36 MPa.



Local misorientation maps were created using EBSD analysis for two specimens, a large and a small radius specimen, both tested at 800°C, 80 MPa. The small radius specimen (see Figure 17) showed signs of high deformation near the notch tip; however, in the center of the gauge, very little deformation was observed. For the large radius specimen (see Figure 18), deformation was observed throughout the thickness of the gauge. This analysis, however, is complicated by the presence of creep damage which relieves stress where voids/cracking occur.

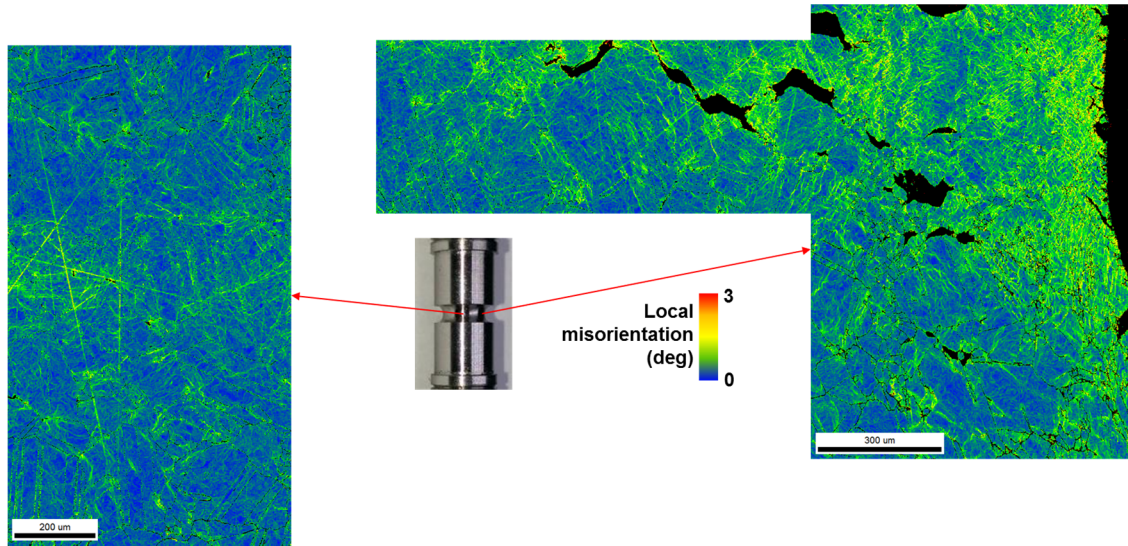


Figure 17. EBSD local misorientation analysis of the small radius U-notch specimen tested at 800°C, 80 MPa.

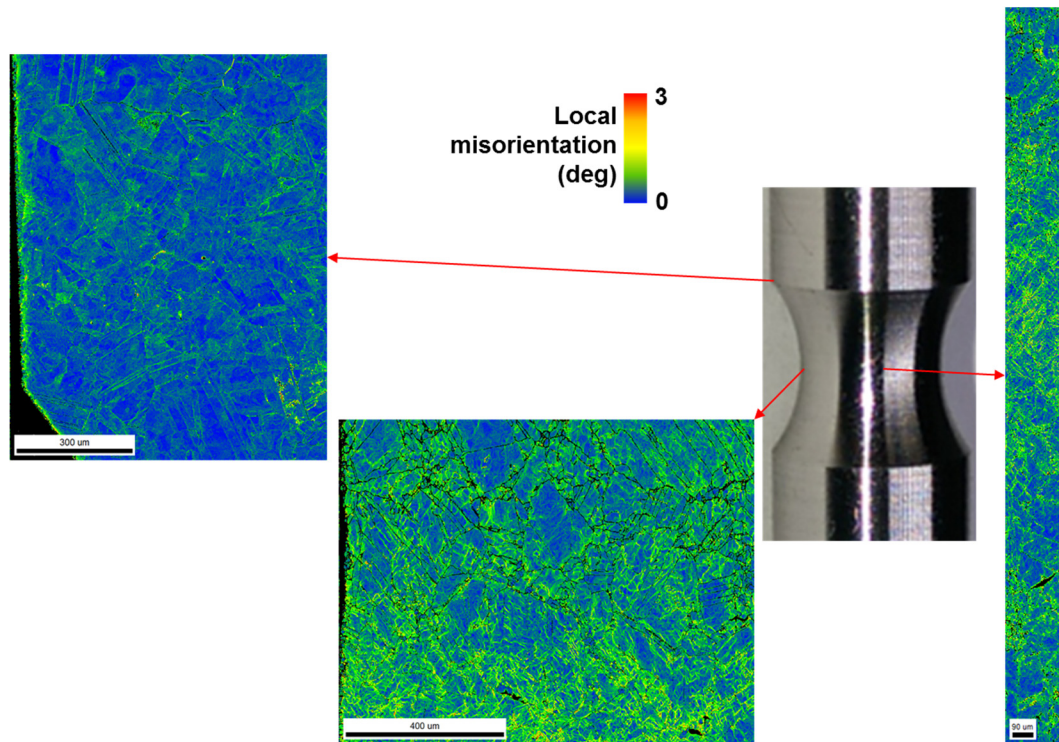


Figure 18. EBSD local misorientation analysis of the large radius U-notch specimen tested at 800°C, 80 MPa.

Analysis of the damage in the cross-section and the local misorientation show that the large radius U-notch specimens, despite having a diffuse multi-axial stress state that extends throughout the thickness of the specimen, behave nearly identically to the straight-gauge, uniaxial stress creep specimens. This is further supported by the similarities in creep-rupture-life of the large radius U-notch specimens and the straight-gauge specimens, as seen in Figure 12. The small radius U-notch specimens, however, show deformation and damage localized in the area near the notch tip, where the multi-axial stress states are strongest. However, despite this damage, the overall rupture life of the small radius U-notch specimen is longer than other tests performed at INL. The multi-axial stress state is not detrimental to overall creep-rupture-life when compared to typical uniaxial stress laboratory tests.

The purpose of the U-notch specimens was to understand the effects of multiaxial stress states. However, these notched specimens do not perfectly simulate a multiaxial applied load. The multiaxial stress state is not constant through the thickness of the specimens, particularly in the small radius U-notched specimens. This raises the concern that the results, which show no decrease in creep rupture life when multiaxial stress states are applied when compared to uniaxial stress states (Figure 12, comparing U-notched specimens to straight gauge), may be a result of the inconsistent multiaxial stress state.

To better understand the effects of stress state and to address the concern that the multiaxial stress state is not constant through the specimen, finite element models were performed at Argonne National Laboratory to depict stress states at the beginning of the test and after creep had been allowed to redistribute the stress. The geometry of the specimen was first modeled and then divided into a mesh, with a finer mesh near the notch, as this is where the multiaxial stress state is applied (See Figure 19). As the specimen is symmetrical, only a quarter of the specimen needed to be modelled to determine the results. Three measurements of stress states were modeled: mean stress, effective stress (Von Mises), and triaxiality ratio. The mean stress is simply the average stress of the three principle stress, calculated as  $\sigma_m = \frac{\sigma_1 + \sigma_2 + \sigma_3}{3}$ . Von Mises stress is calculated as  $\sigma_e = \sqrt{\frac{1}{2}[(\sigma_1 - \sigma_2)^2 + (\sigma_2 - \sigma_3)^2 + (\sigma_3 - \sigma_1)^2]}$ , and the triaxiality ratio is the ratio of the mean stress to the Von Mises stress and is typically used to show the degree of multiaxial stress (a higher number suggest a more multiaxial stress state rather than uniaxial). Examples of these results are shown in Figure 20, Figure 21 and Figure 22. These are summarized in the graph shown in Figure 23, which also includes the maximum principle stress,  $\sigma_1$ .

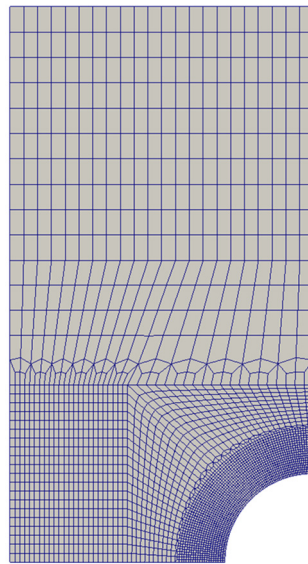


Figure 19. Example of mesh used in finite element analysis.

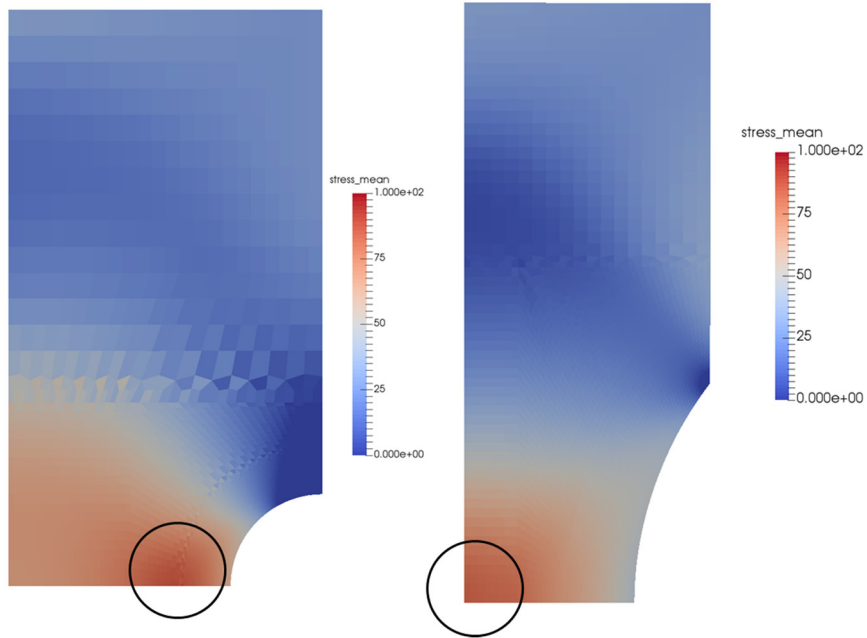


Figure 20. Mean stress after creep has occurred, as calculated for a 750°C 145 MPa creep test for small (left) and large (right) radius U-notch specimens. The maximum value is circled.

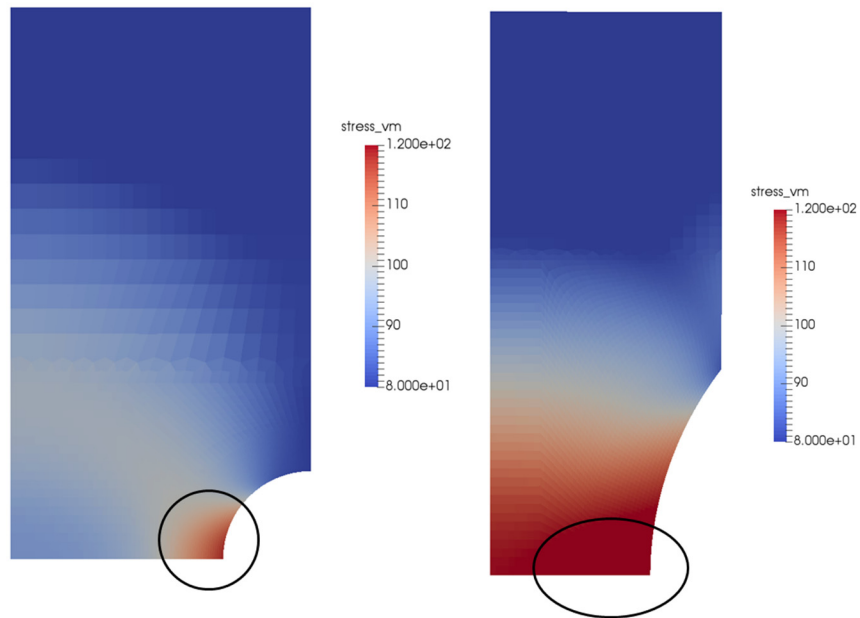


Figure 21. Effective, or Von Mises stress after creep has occurred, as calculated for a 750°C 145 MPa creep test for small (left) and large (right) radius U-notch specimens. The maximum value is circled.

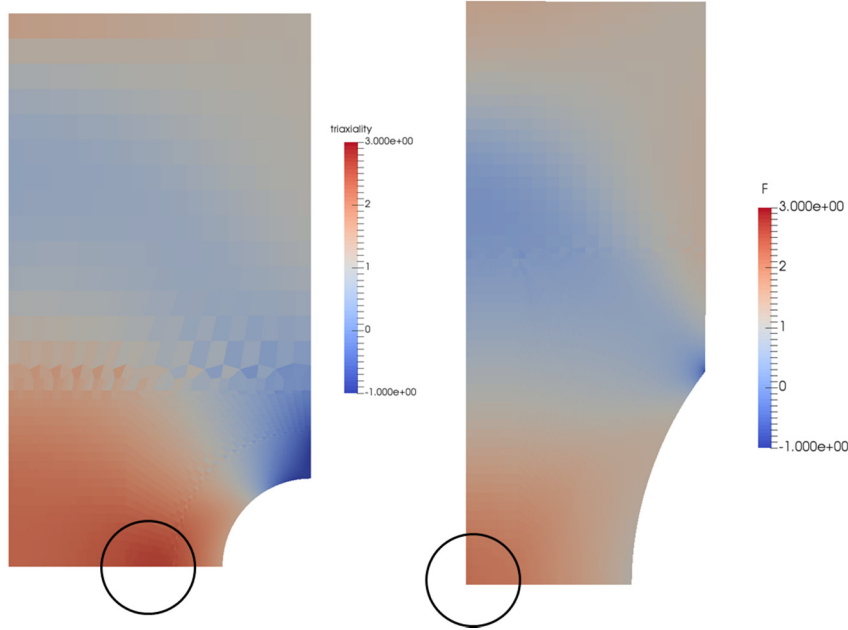


Figure 22. Triaxiality ratio after creep has occurred, as calculated for a 750°C 145 MPa creep test for small (left) and large (right) radius U-notch specimens. The maximum value is circled.

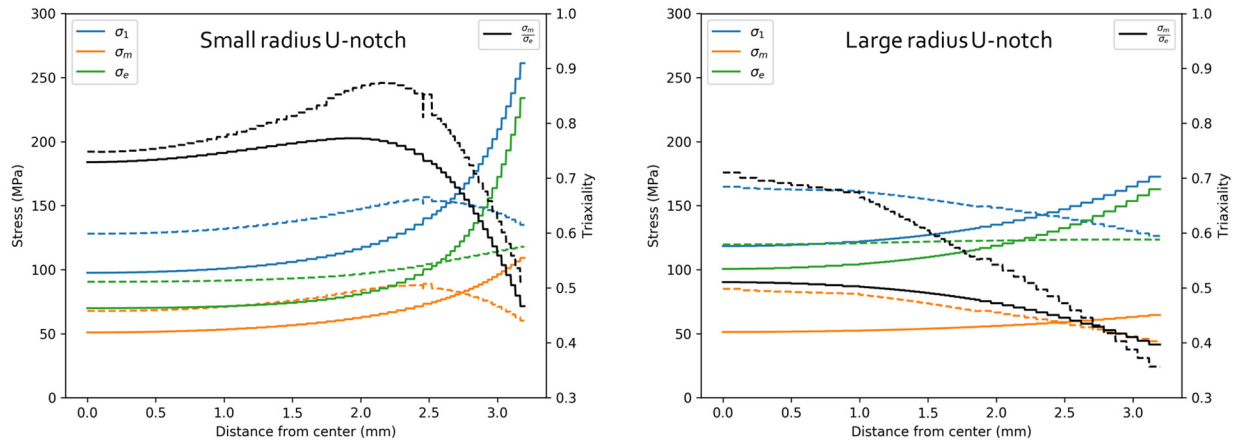


Figure 23. Summary of modelled stress states for 750°C, 145 MPa condition. Solid lines indicate values upon loading the specimen, dashed lines indicate values after creep has occurred.

The goal of this simulation work was to determine if the stress concentrating effects (shown by the high  $\sigma_1$  values near the notch tip – right side of Figure 23) of the notch could be separated out from the multiaxial stress state induced by the notch (shown by the triaxiality). The creep damage of the experimental specimens could then be examined to determine if damage occurred preferentially where the multiaxial stress state was highest (highest triaxiality ratio). If this was not found to occur, then it would strengthen the results suggesting that the multiaxial stress state does not significantly change the creep rupture life over the typical uniaxial creep tests.

In order to apply this to the experimental work, a method was determined for measuring creep damage through the thickness of the specimen. Using a cross section, similar to those shown in Figure 16, pixels in vertical columns were counted as either undamaged metal (grey pixels) or damaged/void areas (black). The fraction of damaged/void to total pixels counted in the column was then used to represent the



degree of damage at that depth into the cross section. This is shown graphically in Figure 24. Areas with little damage, such as the green line, have a very low void fraction. Areas where there is significant creep damage, such as the red line, have a larger void fraction. The void fraction may rise suddenly near the edges (blue and purple line) if a portion of the notch is included in the count.

The results of this analysis are shown in Figure 25 and Figure 26. For the base metal small radius U-notch specimens, the peak damage appears to be just inside from the notch tip, approximately 0.5 mm. For the large radius U-notch specimens, the peak damage occurs in the center, with very little damage occurring within the first millimeter from the notch tip. While these results are not entirely conclusive, a few conclusions may be drawn. The initial stress states (maximum principle stress, mean stress and Von Mises stress) are not relevant to creep damage, as these all peak right at the notch tip prior to creep. After creep has been allowed to occur, the stress states shift. The maximum principle stress and the mean stress peak approximately 0.7 millimeters inside from the notch tip for the small radius specimens and near the center of the specimen for the large radius specimens. The Von Mises stress peak value always occurs near the notch tip, even after creep has occurred, and can therefore be ruled out as not controlling the creep damage which occurs further inside the specimen. After creep has been allowed to occur, the triaxiality ratio peaks approximately one millimeter inside of the specimen from the notch tip for the small radius U-notch specimens, and at the center of the specimen for the large radius U-notch specimens. While not as conclusive, the triaxiality ratio is likely not the factor driving the creep damage. The peak triaxiality ratio is further inside the specimen than where the peak damage is seen in the cross sections of Figure 25. It also has a sharper increase in value as measured from notch tip towards center of the specimen (black dashed line in the right graph of Figure 23), whereas the maximum principle stress and the mean stress approach an almost flat slope towards the center of the specimen (dashed orange and blue lines). This flatter value over a larger area of the center of the specimen matches more closely with the observed damage in Figure 26, where significant damage is viewed over 2-3 millimeters of the center of the specimen. The conclusion from this work confirms that the multiaxial stress state does not significantly change the creep rupture behavior. The use of uniaxial creep rupture results in setting design stress limits is therefore justified.

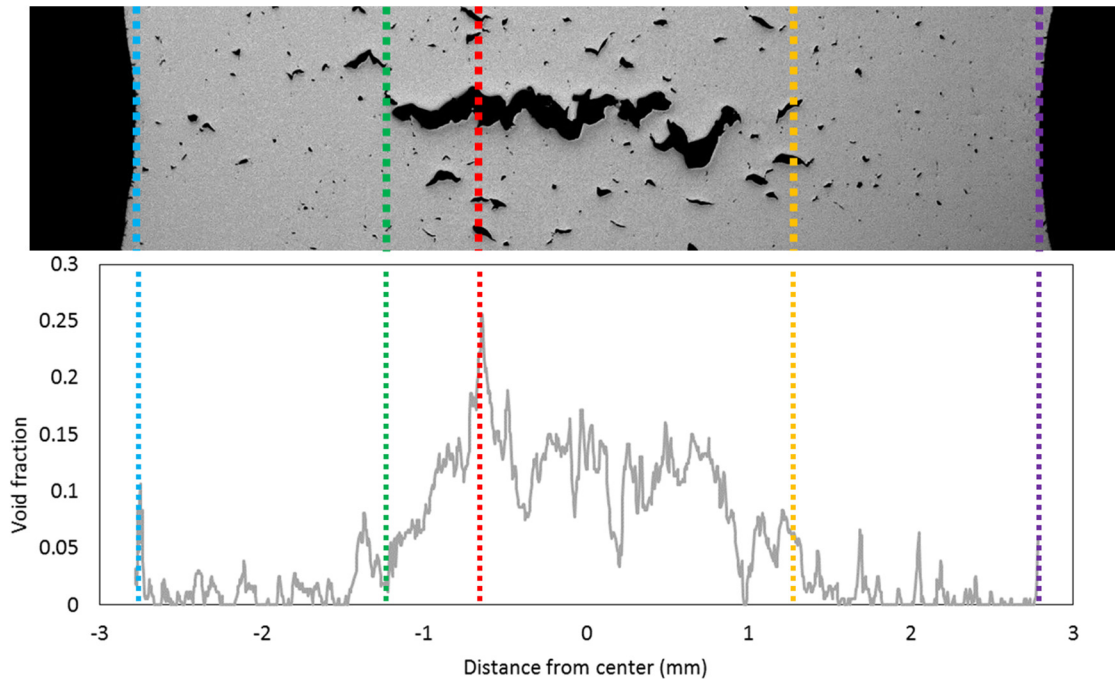


Figure 24. Graphical depiction of the process to determine void fraction (creep damage) vs. depth in the specimen cross section.



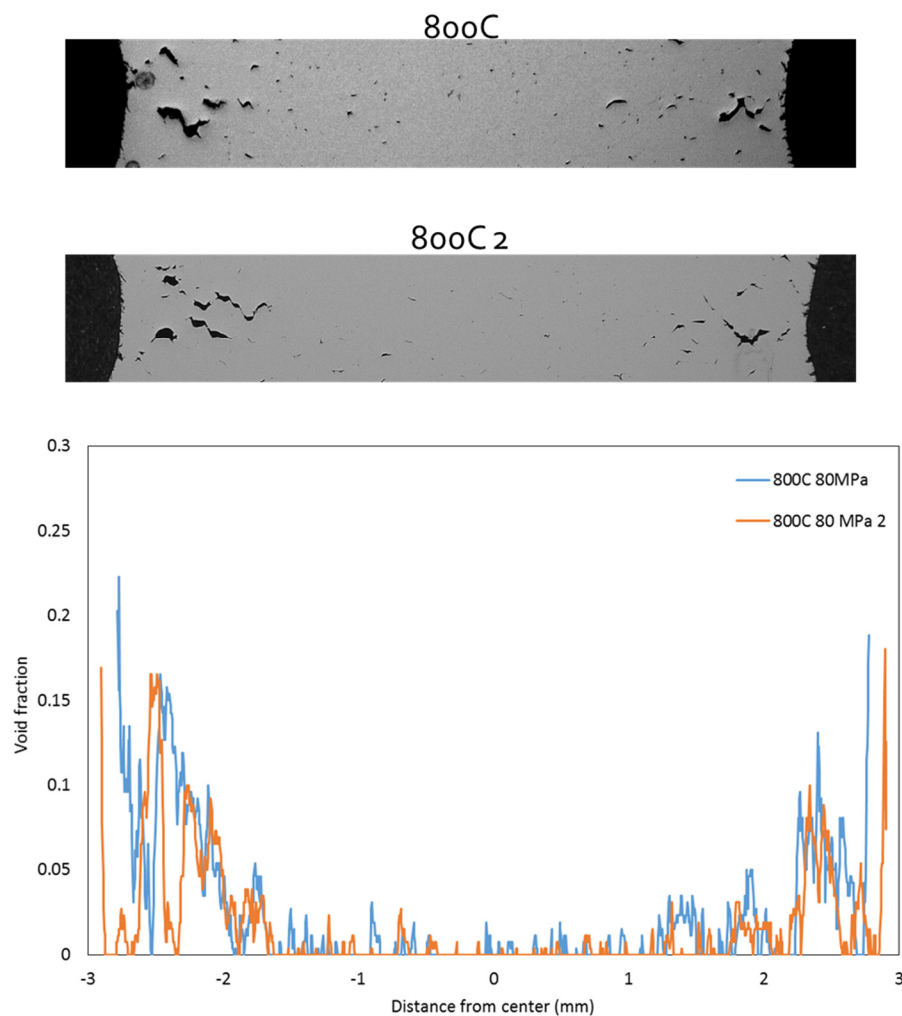


Figure 25. Results of creep damage analysis for two base metal, small radius U-notch specimens tested at 800°C and 80 MPa.

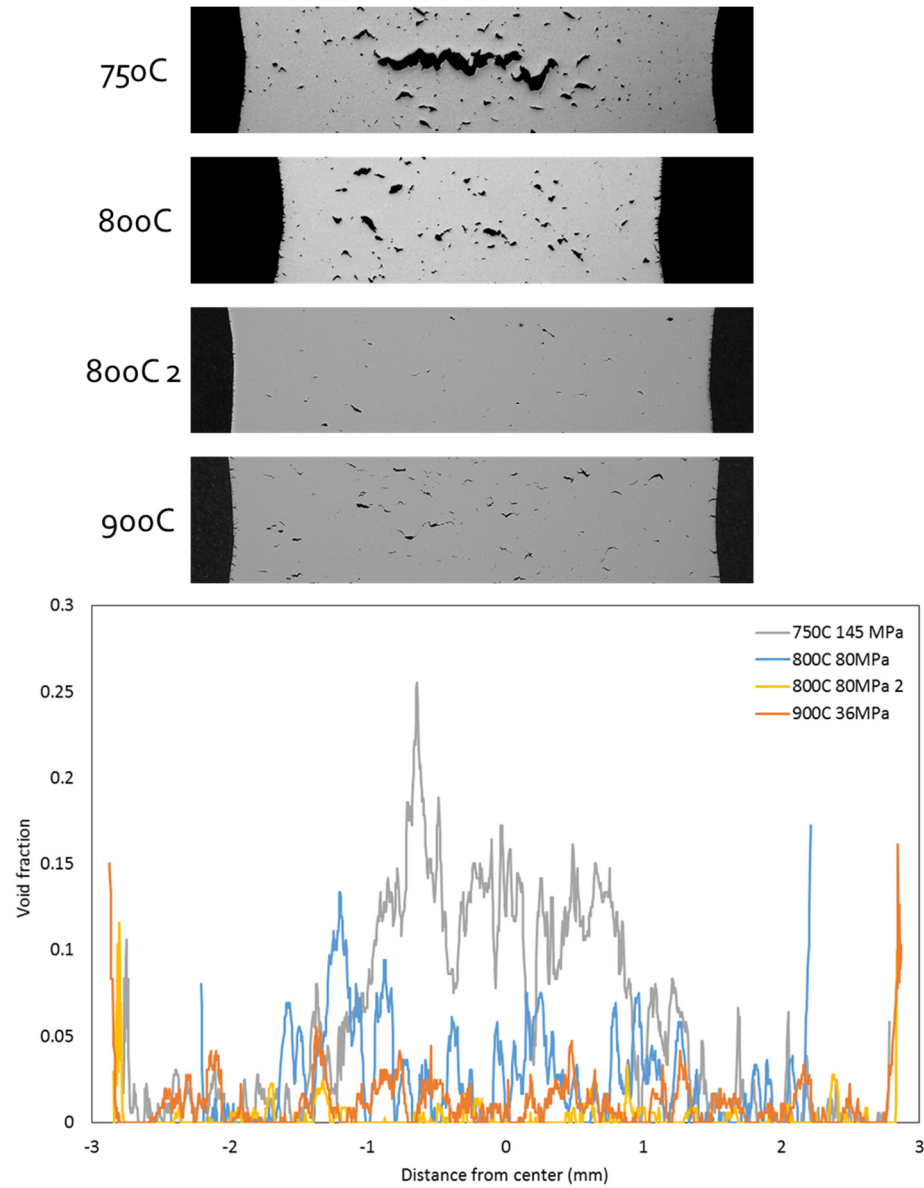


Figure 26. Results of creep damage analysis for base metal, large radius U-notch specimens.

Very little microscopy has been performed on weld metal notched specimens. The first specimen tested, the interrupted 800°C, 80 MPa large radius U-notch specimen, was cross-sectioned and etched to reveal microstructure so that the weld area could be examined with respect to the notched area, shown in Figure 27. It was confirmed through this study that the entire notch was machined within the weld metal.

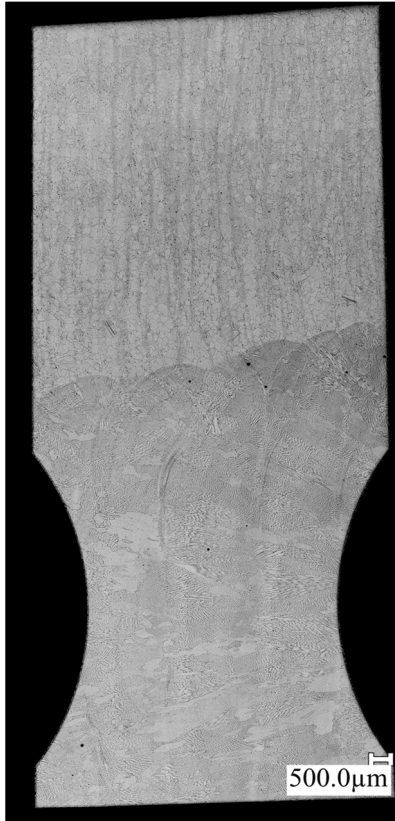


Figure 27. Optical micrograph of an etched cross section from a weld metal large radius U-notch specimen.

### 3.3 Long-Term Testing and Reference Short-Term Specimens

Currently, all notch testing has been performed on a relatively short time scale (1,000 – 10,000 hours). Actual components are expected to see service lives of 30 years (260,000 hours). It is not practical to run creep tests for such an extended time, however, notch strengthening behavior has been modeled to show that it may cross over at low stresses and long times (a material may switch from notch strengthening to notch weakening)[10]. Two long term (100,000 hour expected life) tests have been started at INL, however, to achieve results in a practical amount of time, a method must be determined that can show if the material will fail at the straight gauge or V-notch prior to the end of life. X-ray computed tomography (X-ray CT) has been identified as a technique that will allow for nondestructive evaluation of creep damage so that a specimen may be examined and then the creep test allowed to continue. This was first demonstrated on an unbroken base metal small radius U-notch specimen, shown in Figure 28. Creep damage is visible inside of the specimen and may be measured without destroying the specimen.

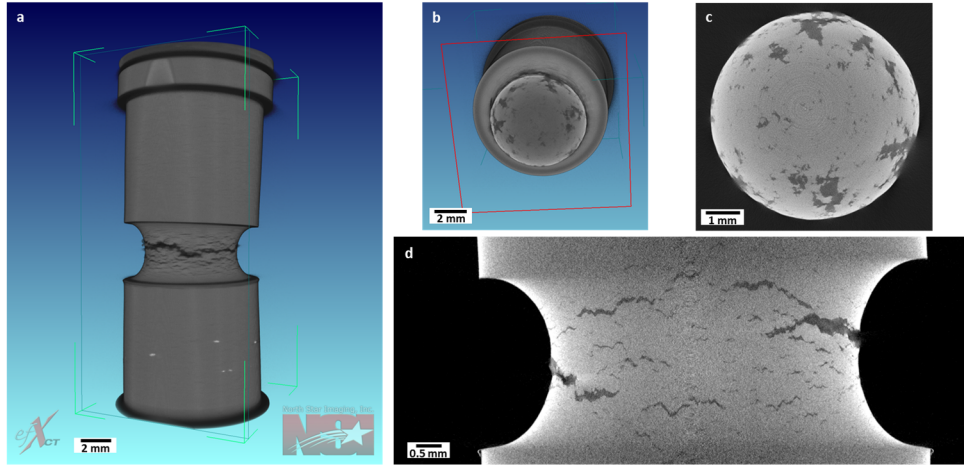


Figure 28. X-ray CT results showing (a) the entire reconstructed specimen, (b) and (c) the circumferential cross section near the root of the notch and (d) the longitudinal cross section. Cross sections were taken from the 3D reconstruction of the X-ray CT results while the specimen remained intact.

This technique will be implemented by examining the X-ray CT results of short-term (1,000–10,000 hour expected lives) test specimens at several stages of the creep test. This will give a baseline of how creep damage begins to occur for notch strengthening material in a reasonable amount of time. These results will then be compared to X-ray CT scans taken periodically of the long term creep specimens. The initial results are shown in Figure 29. The images here are taken at early stages of creep (within 5–10% of the expected creep life) for both a short-term reference weld specimen (Figure 29a and b), as well as the long term base metal specimen (Figure 29c and d). No creep damage is visible at this point of the creep test, though some weld defects may be seen in both the straight gauge and V-notch portion of the weld metal specimen.

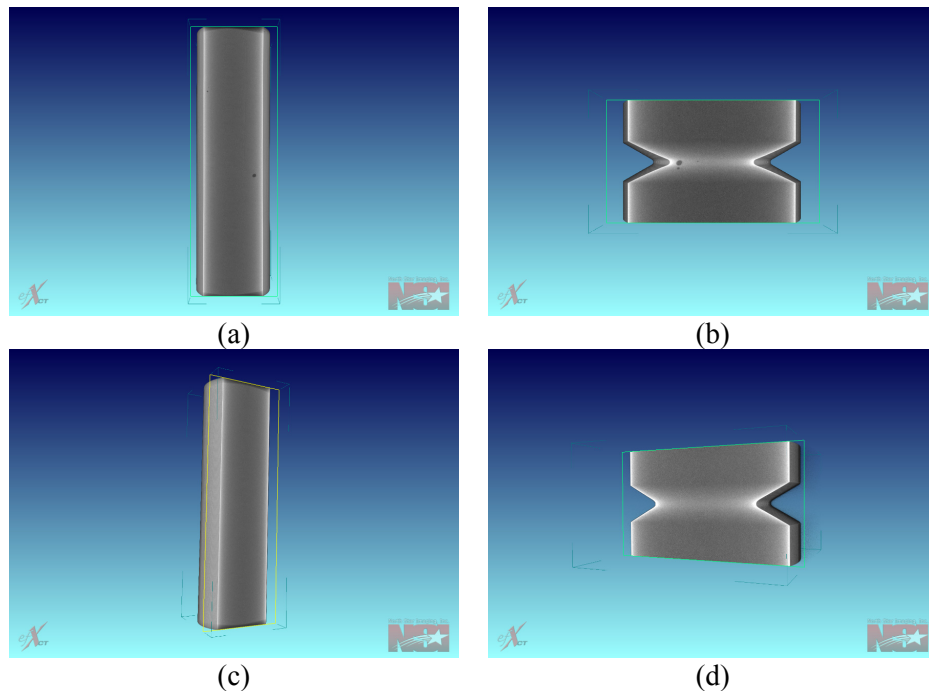


Figure 29. X-ray CT results for the short-term weld metal V-notch specimen (a and b) and the base metal long term V-notch specimen (c and d). Both samples are within 5-10% of their expected lives.

## **4. CONCLUSIONS**

Alloy 617 is a notch-strengthening material for tests performed between 750°C and 1,000°C, with creep-life between 1000–2500 hours. Long term testing has begun to determine if it maintains the notch strengthening characteristic at longer test times. X-ray CT will be used to periodically examine the long term specimens so that the results may be determined prior to the end of the rupture test. Multi-axial stress states do not detrimentally affect creep-rupture-life when compared to uniaxial stress testing. Creep damage appeared to occur in areas of stress concentration (with the highest maximum principle stress and mean stress), rather than the areas with the largest multiaxial stress state (highest triaxiality ratio). Overall rupture life remained unaffected, or was found to increase, in the notched-testing performed in this work. The use of uniaxial test data to set design rules for components that may experience a multiaxial stress state is, therefore, found to be justifiable.

## **5. ACKNOWLEDGMENTS**

The research was sponsored by the U.S. Department of Energy, under Contract No. DE-AC02-06CH11357 with Argonne National Laboratory, managed and operated by UChicago Argonne, LLC. Programmatic direction was provided by the Office of Nuclear Energy.

The authors gratefully acknowledge the support provided by Alice Caponiti, Director, Office of Advanced Reactor Technologies (ART), Sue Lesica, Federal Manager, ART Advanced Materials Program, Hans Gougar of INL, National Technical Director, ART Gas-Cooled Reactors Campaign, and Sam Sham of ANL, ART Technology Area Lead on Advanced Materials.

The authors acknowledge Mark Messner from ANL for the finite element modeling performed in this work, as well as Richard Wright for technical support and Joel Simpson for support maintaining and running laboratory equipment.

## 6. REFERENCES

---

- [1] Wright, R.N., 2018. Updated Draft ASME Boiler and Pressure Vessel Code Case for Use of Alloy 617 for Construction of Nuclear Components for Section III, Division 5, Rev. 1, INL-EXT-17-42999.
- [2] O'Donnell, W.J., A.B. Hull, and S. Malik, 2008. "Structural integrity code and regulatory issues in the design of high temperature reactors," in the Proceedings of the 4th International Topical Meeting on High Temperature Reactor Technology. Washington, DC, USA.
- [3] Wright, R.N., 2016. Test Plan for Evaluation of Notch Effects on High Temperature Rupture Behavior, PLN-5086.
- [4] Webster, G.A., et al., 2004. "A Code of Practice for conducting notched bar creep tests and for interpreting the data," *Fatigue & Fracture of Engineering Materials & Structures*, 27(4): pp.-319-342.
- [5] ASTM E292-09, 2009. Standard test method for conducting time-for-rupture notch tension tests of materials. West Conshohocken, PA, USA.
- [6] ASTM E139-11, 2011. Standard test method for conducting creep, creep-rupture, and stress-rupture tests of metallic materials. West Conshohocken, PA, USA.
- [7] McMurtrey, M.D., et al., 2016. Progress Report on Alloy 617 Notched Specimen Testing, INL/EXT-16-39683.
- [8] Bridgman, P.W., 1952. Studies in large plastic flow and fracture with special emphasis on the effects of hydrostatic pressure. Metallurgy and Metallurgical Engineering Series. McGraw.
- [9] Hertzberg, R.W., 1989. Deformation and fracture mechanics of engineering materials. Wiley.
- [10] Diehl, Sonsino, "Isothermal stress-rupture curves for notched and smooth 617 specimens", Third International Conference on Biaxial/Multiaxial Fatigue, 1989.